This article has been accepted for publication in a future issue of this journal, but has not been fully edited. Content may change prior to final publication. Citation information: DOI 10.1109/TMAG.2015.2451162, IEEE Transactions on Magnetics

Design of Ultra-high Speed Axial Flux Permanent Magnet Machine with Sinusoidal Back-EMF for Energy Storage Application

Sunil Kumar[1], Wenliang Zhao[1], Zhentao S. Du[2], Thomas A. Lipo[3], *Life Fellow, IEEE*, and Byung-il Kwon[1], *Senior Member, IEEE*

[1] Department of Electronic Systems Engineering, Hanyang University, Ansan, Gyeonggi-do, 426-791, South Korea
[2] Department of Electrical and Computer Engineering, University of Wisconsin, Madison WI, USA, 53706
[3] Department of Electrical and Computer Engineering, Florida State University, Tallahassee FL, USA, 32306

This paper focuses on the design and analysis of an ultra-high speed axial flux permanent magnet (AFPM) machine for aerospace flywheel energy storage system. The superiority of the proposed AFPM machine is the material-efficient permanent magnet (PM) shape which contributes to obtain a sinusoidal back-electromotive-force (back-EMF) and hence reduces torque pulsations of the machine such as torque ripple. The harmonics present in back-EMF have a large influence on iron loss and torque pulsations which are always unacceptable in the applications involving the speed as high as 1,000,000 revolutions per minute. Analytical modeling is first performed to determine the PM shape for the proposed models. Then the advantages of the proposed models are verified by comparing with the basic model with conventional ring shaped PMs using 3-D finite element method (FEM). The results show that the proposed models have a nearly ideal sinusoidal back-EMF waveform that significantly reduces the torque ripples compared to the basic model.

***Index Terms*—Axial flux permanent magnet (AFPM) machines, finite element method (FEM), sinusoidal back-EMF, torque pulsations.**

I. Introduction

The use of relatively small-size rotating machines with ultra-high speed has been an area of interest for many emerging applications such as machining spindles, dental drills, compressors and turbochargers, portable power generation, and energy storage systems [1]-[5]. These types of high speed machines possess unique features such as compact size, small number of poles, use of high-energy permanent magnets (PMs), and simple winding arrangement depending upon their specific application. Such machines are being designed to operate at speeds reaching as much as one-million revolutions per minute (1,000,000 rpm) [2]. At such a high speed, machine performance in terms of torque pulsations and losses must be minimized to ensure its smooth operation and high performance.

A significant amount of work has been done concerning ultra-high speed radial flux permanent magnet (RFPM) machines for various applications [1]-[8]. However, for applications such as flywheel energy storage systems, a slotless axial flux permanent magnet (AFPM) machine having a simple air gap winding becomes an attractive option not thoroughly investigated. The inertia of an axial flux machine is easier to adjust than their radial flux counterpart since the thickness of the rotor can be adjusted in axial length without affecting the electromagnetic performance of the machine. A slotless stator core can be formed from a tape-wound core which makes the stator construction much simpler than a radial flux stator which requires a stack of thin punched laminations. Furthermore, a considerable amount of work has recently been done to improve the performance of PM machines by using PM shaping methods [9], [10]. In [10], the authors propose a sinusoidal PM shape that offers the advantages of saving magnet material, reducing torque pulsations and eliminating the unbalanced axial electromagnetic force. This could be a promising alternative for high-performance applications.

In this paper, a novel machine design is presented to achieve a nearly ideal sinusoidal back-EMF by special shaping of the PM, thereby minimizing the torque ripples for aerospace flywheel energy storage systems. Analytical modeling is first performed to determine the required PM shape for the proposed models. Then two proposed models with different stator windings are investigated, with one based on radial winding that validates the analytical modeling and the other based on bunched winding that will be used in the proposed application. To highlight the advantages of the proposed models, a conventional AFPM machine with ring shaped PM is adopted as the basic model. The machine performance characteristics such as back-EMF and electromagnetic torque are predicted by 3-D finite element method (FEM).

II. Proposed AFPM Machine

The proposed design topology utilizes an AFPM machine with a dual rotor and single stator configuration. The conventional annular (ring) shaped magnets that span the entire rotor surface are used in the basic model as shown in Fig. 1. The outer diameter of the stator is fixed at 50 mm while the inner diameter is optimized to give the maximum output torque. The machine has two-phase winding and two permanent magnet poles on each rotor. The design specifications of the machine are listed in Table I.

Manuscript received March 20, 2015. Corresponding author: Byung-il Kwon (e-mail: bikwon@hanyang.ac.kr).
Digital Object Identifier inserted by IEEE

This article has been accepted for publication in a future issue of this journal, but has not been fully edited. Content may change prior to final publication. Citation information: DOI 10.1109/TMAG.2015.2451162, IEEE Transactions on Magnetics

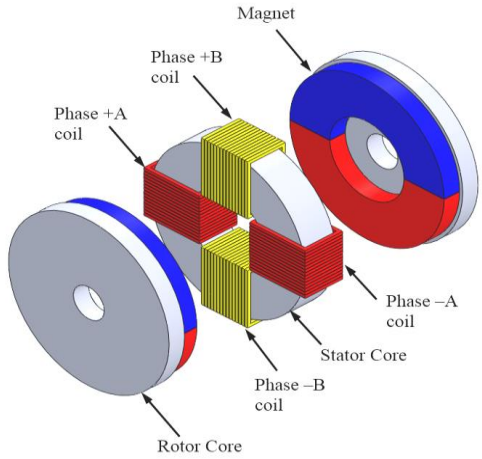

Fig. 1. Expanded view of the basic model.

TABLE I
MACHINE DESIGN SPECIFICATIONS

Item	Unit	Value
Stator outer diameter	mm	50
Stator inner diameter	mm	24
Rotor core outer diameter	mm	52
Rotor core inner diameter	mm	10
Air gap between rotor magnet and stator coil	mm	0.5
Stator core thickness	mm	10
Rotor core thickness	mm	5
Magnet thickness	mm	5
Number of phases	-	2
Number of coils per phase	-	2
Number of turns per coil	-	15
Peak current density	A/mm^2	10
Rotor angular speed	rpm	1,000,000

The inner and outer radial dimensions of the magnet (R_i and R_o) are maintained equal to the corresponding inner and outer dimensions of the stator core, and the airgap length between the rotor and stator is kept as small as possible in order to safely assume that the magnetic field vector ' $\vec{B}$ ' should remain axially directed towards the stator. In this manner, the tangential velocity vector ' $\vec{v}$ ' of the rotor and the magnetic field vector in the airgap are always perpendicular to each other. The analytical modeling of PM shape which induces the back-EMF in the machine is explained below.

The instantaneous back-EMF induced in a single thin conductor can be given as:

$$V(t) = \int_{R_i}^{R} (\vec{v} \times \vec{B}).d\vec{r} \qquad (1)$$

where ' R ' is the radial length of the magnet outer boundary as defined in Fig. 2. Evaluating the right side of (1), we obtain

$$V(t) = \int_{R_i}^{R} vBdr$$

Here, the tangential velocity can be re-written in terms of angular velocity ' ω ' as

$$v = \omega r$$

Therefore, (1) becomes

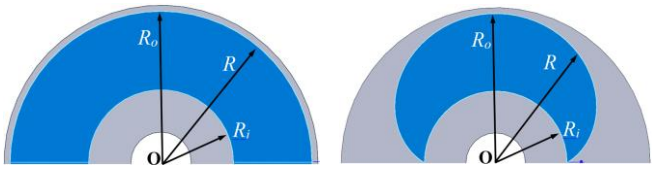

(a) (b)

Fig. 2. Investigated rotor magnet shapes. (a) Basic model rotor with a ring shaped magnet. (b) Proposed model rotor with a sinusoidal shaped magnet.

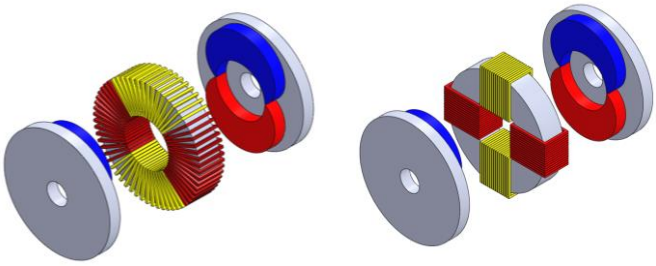

(a) (b)

Fig. 3. Proposed models with sinusoidal magnet rotors. (a) Proposed model 1 with radial winding. (b) Proposed model 2 with bunched winding.

$$V(t) = \omega B \int_{R_i}^{R} r dr$$

$$\Rightarrow V(t) = [\omega B / 2](R^2 - R_i^2) \qquad (2)$$

This result is a general equation for the back-EMF, which is defined by two variables '*B*' and '*R*'. The variable *R* defines the shape of the magnet to be discussed in the following sections. One is the conventional ring shaped magnet, while the other is the sinusoidal magnet shape.

A. *Ring Shaped Magnet*

The back-EMF induced in a single thin conductor due to the conventional ring-shaped magnets, as shown in Fig. 2(a), is defined by

$R = R_o$ for $0 < \theta < \pi$, and

$B(r) = B_0$ for $R_i < r < R_o$

where ' B_0 ' is the airgap flux density which is axially directed from the magnet to the stator core in case of north-pole magnet and vice-versa in case of south-pole magnet. Therefore (2) becomes

$$V(t) = [\omega B_0 / 2](R_o^2 - R_i^2) \qquad (3)$$

After substituting the corresponding values, we obtain the required voltage induced in a stator conductor for a period of one half-cycle. For the remaining half-cycle, the value of airgap flux density becomes negative as the conductor comes under the influence of the south-pole. In this case the back-EMF obtained is negative and the resultant waveform becomes a square wave over one-cycle.

B. *Sinusoidal Shaped Magnet*

To obtain the desired sinusoidal back-EMF waveform a sinusoidal PM shape can be designed as shown in Fig. 2(b), which is defined by

This article has been accepted for publication in a future issue of this journal, but has not been fully edited. Content may change prior to final publication. Citation information: DOI 10.1109/TMAG.2015.2451162, IEEE Transactions on Magnetics

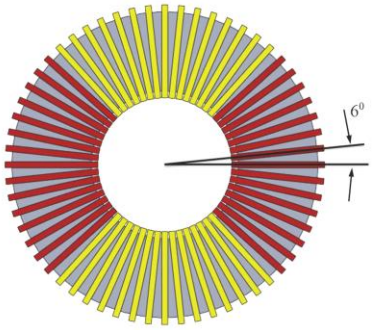

Fig. 4. Radially wound stator for proposed model 1.

$B(r) = B_0$ for $R_i < r < R$, and
$B(r) = 0$ for $R_i > r > R$. Also,
$V(t) = 0$ when $R = R_i$, and
$V(t) = V_{\max}$ when $R = R_o$. Therefore,

$$V_{\max} = [\omega B_0 / 2](R_o^2 - R_i^2).$$

Thus, the factor $(R^2 - R_i^2)$ in (2) must vary in the form $[(R_o^2 - R_i^2)\sin\theta]$ to obtain a sinusoidal voltage. i.e.,

$$(R^2 - R_i^2) = (R_o^2 - R_i^2)\sin\theta$$

$$\Rightarrow R = \sqrt{(R_o^2 - R_i^2)\sin\theta + R_i^2} \quad (4)$$

which is the required equation for a sinusoidal shaped magnet. The induced voltage now becomes

$$V(t) = [\omega B_0 / 2](R_o^2 - R_i^2)\sin\theta. \quad (5)$$

This equation now demonstrates that a sinusoidal voltage can be induced in a thin conductor using the sinusoidal shaped magnet. The two proposed models with different stator windings are shown in Fig. 3. The proposed model 1 with radial winding is shown in Fig. 3(a), and the proposed model 2 with bunched winding is shown in Fig. 3(b). In Fig. 3(a), the stator winding is designed with thin conductor turns of practical width with the radial distribution. Each turn is separated by an angle of 6-degrees electrical as well as mechanical as shown in Fig. 4. In this configuration, the induced sinusoidal voltage in each phase will be given as:

$$V_{phase} = n_{ct} n_{cp} \sum_{n=-7}^{7} [V_{\max} \sin\{\theta + (6n\pi / 180)\}] \quad (6)$$

where n_{ct} is the number of conductors per turn, and n_{cp} is the number of coils per phase. (n_{ct} = 2 and n_{cp} = 2 in our case).

III. FEM Results and Analysis

In order to analyze the electromagnetic performance of the investigated models, three dimensional finite element method (FEM) is utilized. The analytical modeling is verified through FEM analysis by using the proposed model 1 since the winding used in this model is radial winding, which realizes

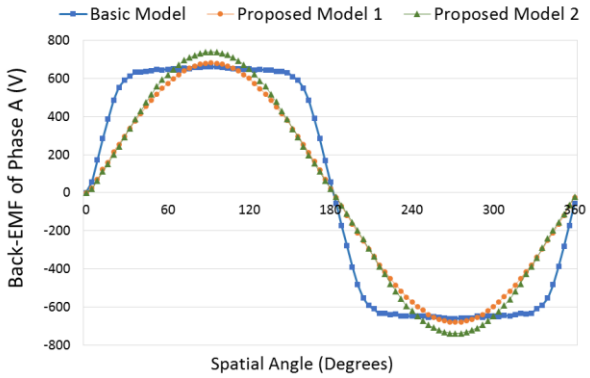

Fig. 5. Back-EMF comparison.

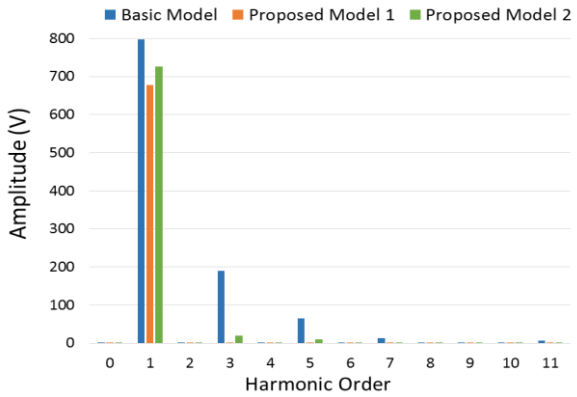

Fig. 6. Back-EMF FFT comparison.

the analytical formulation explained in the previous section. The back-EMF induced in each turn of the coil is a sine wave but phase shifted from each other as governed by (6). However, the resultant back-EMF of the coil will remain sinusoidal as the sum of all sine waves of same period but phase shifted from each other results in a sine wave irrespective of their amplitudes. 3-D FEM results show that a near ideal sinusoidal back-EMF with total harmonic distortion (THD) factor of 0.64% can be achieved in case of proposed model 1. The back-EMF THD factor can be calculated by using the formula:

$$THD = \frac{\sqrt{V_2^2 + V_3^2 + V_4^2 + \ldots}}{V_1} \quad (7)$$

where 'V_1' is the fundamental component of the back-EMF.

In practice, however, the application of such machines could require the winding to be inserted in bunched coil fashion as shown in Fig. 3(b) which is designated as the proposed model 2. This introduces the harmonics in the back-EMF of the proposed model 2 with a THD of 3.10%, which is still considerably better when compared to the basic model with back-EMF THD factor of 25.27%.

The back-EMF comparison of phase-A of all the three models is shown in Fig. 5. The back-EMF waveform of proposed model 1 and proposed model 2 is much closer to the sinusoidal waveform. Fig. 6 shows the corresponding Fourier transforms in which the 3rd, 5th, and 7th harmonic components have almost been eliminated in case of proposed model 1 and

This article has been accepted for publication in a future issue of this journal, but has not been fully edited. Content may change prior to final publication. Citation information: DOI 10.1109/TMAG.2015.2451162, IEEE Transactions on Magnetics

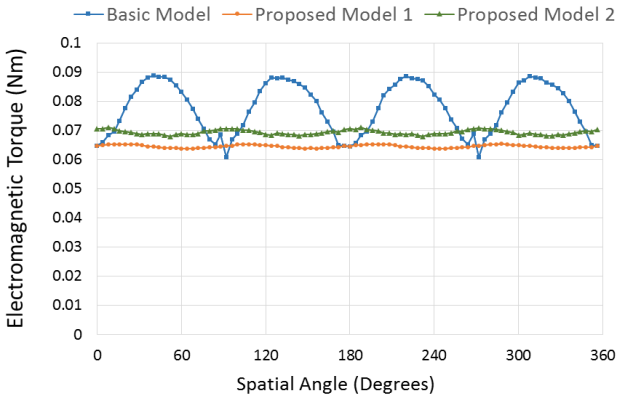

Fig. 7. Electromagnetic torque comparison.

Fig. 8. Electromagnetic torque FFT comparison.

TABLE II
3-D FEM RESULTS COMPARISON

Item	Unit	Basic Model	Proposed Model 1	Proposed Model 2
Back-EMF (THD factor)	%	25.27	0.64	3.10
Back-EMF (RMS value)	V	581.1	479.1	513.9
Electromagnetic torque (Average)	Nm	0.0777	0.0645	0.0694
Torque ripple factor	%	35.99	2.50	4.75

proposed model 2. Fig. 7 shows the electromagnetic torque comparison of the models. The torque ripples are suppressed in proposed models as expected from the sinusoidal back-EMF. The torque ripple factor (TRF), defined as the ratio of peak-to-peak torque to the average torque, is calculated as:

$$TRF = \frac{T_{MAX} - T_{MIN}}{T_{AVG}} \quad (8)$$

The torque ripple factor of the basic model and the proposed model 2 is found to be 35.99% and 4.75% respectively which shows about 86.8% reduction in torque ripples. The FFT analysis of the torque is performed in Fig. 8 which shows that the 4th and 8th harmonics have been greatly suppressed as expected from the back-EMF THD value. The overall comparison of the investigated models is listed in Table II, which shows the machine performance in terms of torque ripples is much improved. The proposed sinusoidal PM shape has 36% reduced magnet volume than the conventional ring shaped PMs. The average torque is slightly decreased in proposed models but the torque density has been increased. However, our basic design target is high energy density which will be achieved from the high speed rotating mass of the machine.

IV. CONCLUSION

A small-size and ultra-high speed AFPM machine has been introduced in this paper to improve the performance in terms of back-EMF and torque pulsations for aerospace flywheel energy storage systems. The rotor PM shape is designed to obtain a sinusoidal back-EMF using analytical modeling. Based on two types of winding, two models are proposed utilizing the sinusoidal magnets. Then a 3-D FEM analysis has been performed which validates that the proposed sinusoidal models have much less back-EMF harmonics and torque ripple than the basic model. As a future prospect, machine performance in terms of mechanical and thermal stress will be considered and experimental work will be implemented.

ACKNOWLEDGMENT

This research was jointly supported by the BK21PLUS program through the National Research Foundation of Korea funded by the Ministry of Education, and the Human Resources Program in Energy Technology of the Korea Institute of Energy Technology Evaluation and Planning (KETEP), granted financial resource from the Ministry of Trade, Industry and Energy, Republic of Korea (20154030200730).

REFERENCES

[1] W. Wang, H. Hofmann, and C. E. Bakis, "Ultrahigh Speed Permanent Magnet Motor/Generator for Aerospace Flywheel Energy Storage Applications," *IEEE Int. Conf. Electr. Mach. Drives*, vol., no., pp.1494,1500, 15-15 May 2005.

[2] C. Zwyssig, J. W. Kolar, and S. D. Round, "Megaspeed Drive Systems: Pushing Beyond 1 Million r/min," *IEEE/ASME Trans. Mechatronics*, vol.14, no.5, pp.564,574, Oct. 2009.

[3] C. Zwyssig, M. Duerr, D. Hassler, and J. W. Kolar, "An Ultra-High-Speed, 500000 rpm, 1 kW Electrical Drive System," *in Proc. Power Convers. Conf., Nagoya, Japan 2007. PCC '07* , vol., no., pp.1577,1583, 2-5 April 2007.

[4] A. Tuysuz, C. Zwyssig, and J. W. Kolar, "A Novel Motor Topology for High-Speed Micro-Machining Applications," *IEEE Trans. Ind. Electron.*, vol.61, no.6, pp.2960,2968, June 2014.

[5] D. Krähenbühl, C. Zwyssig, H. Weser, and J. W. Kolar, "A Miniature 500 000-r/min Electrically Driven Turbocompressor," *IEEE Tran. Ind. Appl.*, vol.46, no.6, pp.2459,2466, Nov.-Dec. 2010.

[6] D. W. Swett and J. G. Blanche IV, "Flywheel charging module for energy storage used in electromagnetic aircraft launch system," *IEEE Trans. Magn.*, vol.41, no.1, pp.525,528, Jan. 2005.

[7] D. K. Hong, B. C. Woo, J. Y. Lee, and D. H. Koo, "Ultra High Speed Motor Supported by Air Foil Bearings for Air Blower Cooling Fuel Cells," *IEEE Trans. Magn.*, vol.48, no.2, pp.871,874, Feb. 2012.

[8] L. Zhao, C. Ham, L. Zheng, T. Wu, K. Sundaram, J. Kapat, and L. Chow, "A Highly Efficient 200 000 RPM Permanent Magnet Motor System," *IEEE Trans. Magn.*, vol.43, no.6, pp.2528,2530, June 2007.

[9] S. Q. A. Shah, T. A. Lipo, and B. I. Kwon, "Modeling of Novel Permanent Magnet Pole Shape SPM Motor for Reducing Torque Pulsation," *IEEE Trans. Magn.*, vol.48, no.11, pp.4626,4629, Nov. 2012.

[10] W. Zhao, T. A. Lipo, and B. I. Kwon, "Material-Efficient Permanent-Magnet Shape for Torque Pulsation Minimization in SPM Motors for Automotive Applications," *IEEE Tran. Ind. Electron.*, vol.61, no.10, pp.5779,5787, Oct. 2014.